Experimental determination of the thermal performance of a free standing fin Structure copper heatsink

Jan Bijan Pourian

PhD student, Dept. of Public Technology, Mälardalen University, MdH

jan.pourian@mdh.se

Mark Irwin

Manager Director of the TPC AB at halstahammar, Sweden

PhD, Outokumpu R&d

mark.irwin@tpcab.se

Jafar Mahmoudi phd at mdh & Outokumpu

jafar.mahmoudi@mdh.se

1. Abstract

New design, experimental and numerical efforts, optimization and manufacturing process constitute the elements of investigation of this paper.

The fundamental objective of the present study is to compute the thermal dissipation capability of a new design constructed for copper heatsinks and also deals with challenges in manufacturing of these components.

A part of experimental efforts are conducted to estimate the thermal characteristic of the offered heatsink.

The numerical analysis is performed to generally predict the effect of thermal conductivity of materials on the heat dissipation rate by heatsinks.

Optimization by experimental approach is also conducted to evaluate the flow parameters and to establish a compromise between the characteristics of the flow regime and the geometric identity of the design.

Numerical investigation is performed by CFD to evaluate and compare heat dissipation capabilities of aluminium and copper heatsinks.

Manufacturing solutions are proposed which would facilitate fabrication of more high performance copper heatsinks. The intention is to illustrate the potential of copper cooling components to meet increasing demands for smaller and more powerful processors, which require greater heat dissipation. Efforts are focused to design an easily manufactured heat sink with enhanced thermal performance while minimizing variables such as weight and cost.

A copper heat sink with superior thermal characterisation is designed based on the theoretical analysis of the numerical efforts as well as manufacturability concerns. Comparison of the thermal characteristic of both the proposed copper design and a typical aluminium heatsink was then performed under identical experimental conditions. At the first phase of the experimental efforts, we compared thermal capability of 5 different aluminium (plate and pin fins) heatsinks using in the computers. The best aluminium heatsink based on the maximum thermal capacity criteria is selected. The copper heat sink design arrived upon in this study consists of an array of copper fins 0.2mm in thickness. This design was compared with an aluminium heatsink designated for AthlonXp 2800+.

2. Nomenclature

A   surface area / cross section area (m2)

D   diameter

K_{eff} effective conductivity

h   Heat transfer coefficient /enthalpy

$\bar{J}_j$ Diffusion flux of species j

P   power /pressure

P_d Dynamic pressure

P_e Performance
P_s Static pressure
P_t Total pressure
Δp Pressure difference
q   Heat rate
$\dot{q}$ Heat generation
q'' Heat flux
R   Pipe radius
Re   Reynolds number
S_h heat of chemical reaction
ΔT Temperature difference
T_r Room temperature
T_{sou} Source temperature
T   Temperature
U_D Average velocity in pipe
U_y Air velocity, air velocity at
        Distance y from the wall
V   Volume
U_{max} Maximum air velocity (in the centre)
y   Distance from the wall
ρ Air density
υ Kinematics' viscosity of air
μ Dynamic viscosity of air

3. Introduction

The heat generation in electronic devices is increasing due to acceleration of advances in performance of novel computers. Ejection of the generated heat in electronic components is becoming a more deep challenge. Heatsinks have been the exclusive solution for removing the heat from the sources of heat in electronic devices. But enhancement of generated heat in electronic components advances continuously in which impose improvement of the current heatsinks. Development of the heatsinks is managed by treating the physical parameters that influence the thermal characteristics of the applied materials in heatsinks and also parameters of convective heat transfer and flow regimes. The influence of the materials of heatsinks in the heat transfer problems is an indisputable subject. The impact of the materials of heatsinks is respected by

introducing the thermal conductivity of the materials.

Thermal conductivity is one of the parameters that are directly proportional the rate of heat transfer by conduction.

Although copper has a thermal conductivity that is about two times greater than that of aluminium, but still the aluminium heatsinks are more commonly used today for heat dissipation in computers. (K_{Al}= 237 W/m k, K_{Cu}= 401W/m k).

In this study the existent obstacles in the path of production process of copper heatsinks are investigated.

3.1 Challenges in manufacturing of copper heatsink

Three challenges for manufacturing of copper heatsinks are supposed including, weight, hardness and thickness. These physical and geometrical variables make fabrication of copper heatsinks difficult at different manufacturing process such as casting, laser and water cutting.

At the present time, casting and cutting are not a viable fabrication method for thin fin and light copper heatsinks.

4. Theoretical approach

Volumetric flow rate
Inlet air velocity can be measured base on the specification and dimension of the fan.

$$Q = A.\,U \tag{1}$$

Pitot tube correlation
According to Bernoulli's equation:
Static pressure +dynamic pressure = total pressure

$$P_s + \frac{\rho U^2}{2} = P_t$$

$$U^2 = \frac{2(P_t - P_s)}{\rho} \tag{2}$$

The pressure transducer measures the difference in total and static pressure, which is dynamic pressure.

Dynamic pressure $= P_d = 1/2\,\rho U^2$ (3)

Reynolds number
Reynolds number applies as a criterion to distinguish the airflow regimes blowing the heatsink.

$$R_e = \rho U_D D \Big/ \mu \quad or \quad R_e = \frac{UD}{\nu}$$ (4)

Re<2300, smooth pipes: laminar flow
4000<Re <80000, smooth pipe: Turbulent flow.

Analytical calculation of velocity distribution laminar flow

$$\frac{U_y}{U_{max}} = 1 - \left(\frac{y}{R}\right)^2$$ (5)

Analytical calculation of velocity distribution turbulent flow

$$\frac{U_y}{U_{max}} = 1 - \left(\frac{y}{R}\right)^n$$ (6)

Convective heat transfer

$$q = hA(\Delta T)$$ (7)

Reduced thermal energy equation applied by CFD for heatsinks

$$\nabla.(\vec{v}(\rho E + p)) = \nabla.\left(k_{eff}\nabla T\right)$$ (8)

Relative performance

We employed the following relation to compare the thermal performance of the heatsinks under the same conditions.

$$Max.T_{SOU} = T_r + (P_e)(P)$$ (9)

Transport equations for the standard k-ε model
Turbulent kinetic energy and the rate of dissipation, ε, are obtained from the following transport equations:

$$\frac{\partial}{\partial t}(\rho k) + \frac{\partial}{\partial x_i}(\rho k u_i) = \frac{\partial}{\partial x_j}\left[\left(\mu + \frac{\mu_t}{\sigma_k}\right)\frac{\partial k}{\partial x_j}\right] +$$
$$G_k + G_b - \rho\varepsilon - Y_M + S_k$$ (10)

$$\frac{\partial}{\partial t}(\rho\varepsilon) + \frac{\partial}{\partial x_i}(\rho\varepsilon u_i) = \frac{\partial}{\partial x_j}\left[\left(\mu + \frac{\mu_t}{\sigma_\varepsilon}\right)\frac{\partial\varepsilon}{\partial x_j}\right] +$$
$$C_{1\varepsilon}\frac{\varepsilon}{k}(G_k + C_{3\varepsilon}G_b) - C_{2\varepsilon}\rho\frac{\varepsilon^2}{k} + S\varepsilon$$ (11)

The performance of the proposed heatsink design is compared with several standard heatsinks. Presenting an absolute thermal dissipation capability of a heatsink is complicated. In addition to those parameters that we use to evaluate relative performance, the absolute heat performance can be a function of the parameters like the type of source material, cross section area, weight, and surface area, type of the fan and test conditions. The relative performance of the reference heatsink according to common rules is known and accessible.

5. Experimental works

5.1 Heatsink design
The new design pivots around observations from the earlier numerical investigation that will be discussed in the numerical results section.
The geometry and final dimension of the fins for the proposed copper heatsink is shown in the following figures.
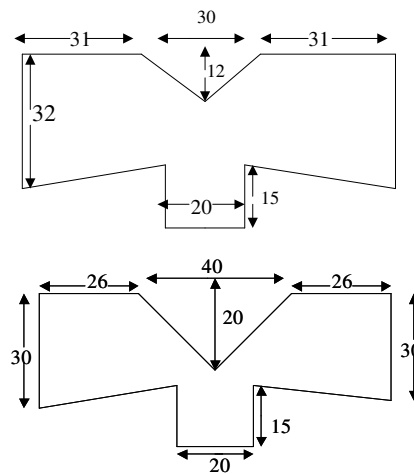
Figure 1: Proposed geometries for the plates

5.2 Construction

The heatsink was constructed by mechanically bundling together 35 fins of the design shown in the figure (1).
The thickness and the length of the fins is respectively 0,2 mm and 92 mm. The fins are bent from both sides and from zero to 180 degrees horizontally in the X-Z plane respectively from the centre fin to the last fins at both sides of the component. The weight of the heatsink varies in the range of 170-200 grams depending on the applied proposed fins.

Figure 2: The proposed inclined heatsink

5.3 Measurement procedures and equipments

The fan used for characterisation of the heatsink is A0812MS-A70GL with the following specifications: DC 12V, 0, 15 A, 80×80×25, 1,8 W, volumetric flow rate 31,4CFM. The same fan is used for both heatsinks. A pressure measuring transducer GMUD is employed in combination with a Pitot tube to measure the pressures ahead of and after the heatsink. The temperature is measured by data acquisition 34970A in associated with HP Bench Link program. The adhesive "k" type thermocouple is applied to measure the temperature of the fins and heat source.
An Anemometer Testo 400 measures the air velocity.
Spatial fin arrangement of the proposed heatsink is agree with impingement airflow. The fan is located above the heatsink normal to the base. This mode of fan mounting is called TISE (Top-Inlet, Side-Exit).
Thermal performance is determined by applying the initial (room temperature) and maximum temperature of the heat source or the equilibrium temperature at the applied power.

The heat sources are respectively 25, 30, 100 and 100-200 watt resistors of the type Mp725, 1.00 & 1% R and MP930, MP9100, Fabr Arcol (2,2 Ω, dimension: 38,2×30,3×13,5mm). (See attachment)
A 1400 W, SM3540 power supply in the range of 35V × 40A is adopted to run the resistors with different current.

Figure 3: The measurement equipments

6. Modelling and simulation

The numerical efforts are conducted to investigate the influence of the thermal conductivity of materials on the thermal dissipation capability of the heatsinks. Two materials are selected at this phase of the study. Aluminium is selected because the most current heatsinks are constructed by using this material and the copper is adopted as the competitor material that has superior thermal properties. The primary study of aluminium and copper heatsinks is relied on the numerical investigation. Computational fluid dynamic (CFD) is applied to this purpose. Two copper and aluminium heatsink with the same dimension and each one consisting of 48 plates set as two rows on a base are modelled as 3-dimensional in the Gambit and simulated by fluent program.

The map meshing scheme is applied to the volumes, representing the fins and the air flow between them. These volumes have been meshed by arrays of hexahedral mesh elements. For the space over the fins where the air inlets from a channel a T-grid mesh type which is proper for any geometry is adopted. The grid poses totally 497197 cells.

Boundary conditions and continuum zones are specified in the Gambit.
Two major boundary conditions are inlet and outlet flows in this case which are respectively defined as mass-flow-inlet and pressure outlet.
 A wall type of boundary condition is adopted for the heat source. The amount of heat flux generated at this face is $600000 W/m^2$. The heat source is represented in the model as a face at bottom of the sink.
The solid type of continuum zones is adopted for the fins whereas a fluid type is defined for the volumes between the fins, representing the air.
Cooling process is accomplished by impingement force convection. The airflow through a duct above the heatsinks blows the air and cools down the fins.
The energy and viscous models are solved to treat the thermal performance of the heatsinks.
A $k-\varepsilon$ turbulent flow regime is modelled for heatsinks.

7. Results

7.1 *Numerical results*
Several numerical simulation in the fluent framework are conducted to study the impact of the thermal conductivity and to compare aluminium and copper as the constituent materials of the heat sinks.
The flow velocity is also another variable of simulation which is taken into account to analyse the impact of the inlet volumetric flow rate and the

applied powers of the fan on heat removing from the heat generation components. However, the effect of the power of fan is not directly treated but since the cross section area of the flow is hold constant when the flow velocity varies, therefore, any increasing or decreasing of flow velocity may be considered as respectively the elevation and drop of the power. It is worthwhile to note that since the intention is exclusively comparison the thermal characteristics of heatsinks by treating the thermal conductivity, therefore any significant attention is paid to absolute values obtained from the CFD.
The numerical results are shown in the next table.

Material	Velocity m/s	Heat flux W/m^2	Max. Temp. K
Cu	10	1300000	363
Cu	4	1300000	383
Cu	3,4	700000	355
Cu	2	700000	362
Cu	10	600000	338
Cu	3,4	600000	347
Al	10	1300000	433
Al	10	600000	361
Al	3,4	600000	371
Al	3,4	1300000	450
Al	10	1300000	434

Table 1: Numerical results achieved for Al and Cu heatsinks

The numerical demonstration of the bottom plate of the heatsinks after applying a power of $60 w/cm^2$ to the heat source is exposed in figure 4A and 4B. The airflow hits the bottom plate with a velocity of 10 m/s.
As shown in the numerical demonstration there is a heat spreading resistance that leads to a lesser rate of heat on the base of the heatsink at the longer distances from the heat source.
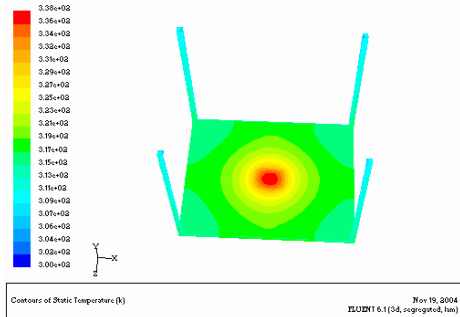
Figure 4A: Demonstration of heat spreading on the copper plate
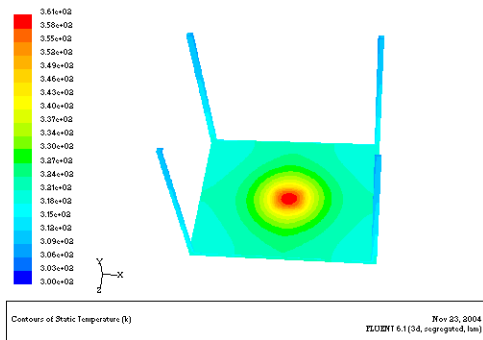
Fig4B: Demonstration of the heat spreading on Aluminium plate the applied power is 60 W/cm² and the air velocity is 10 m/s for both heatsinks

7.2 Experimental results

7.2.1 Relative performance

The heat is generated in a heat source that is attached to the bottom of the heatsink. Volume and cross section area of the source is also given in the table (2). Various powers are applied to the source and the maximum or the equilibrium temperature of the source is measured for both copper and aluminium applications.

q (W)	$V_{source}=$ 1.87E-07m³ $\dot{q}(W/m^3)$	$A_{source}=$ 6.7E-05m² $q''(W/m)$	T_{max} (1)	T_{max} (2)
14	2.67E+07	7.46	31.8	33.9
10.5	2.67E+07	15.67	44.6	47.3
14	7.67E+07	20.89	52	55.9
22.5	1.20E+08	33.58	70.3	78.3

Table 2: Heat dissipation by Copper and aluminium heatsinks from a heat source with a max 37w/cm²

(1) Max temp. of source with Suggested heatsink (ºc)

(2) Max temp. of source with Reference heatsink (ºc)
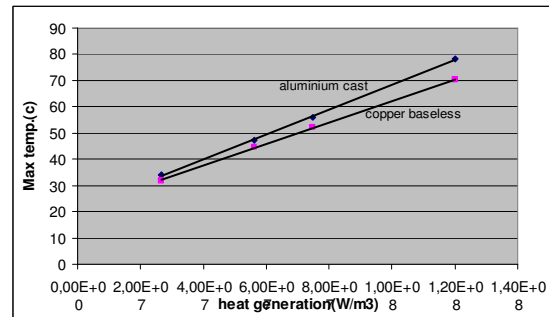
Graph 1: Relative performance MP725
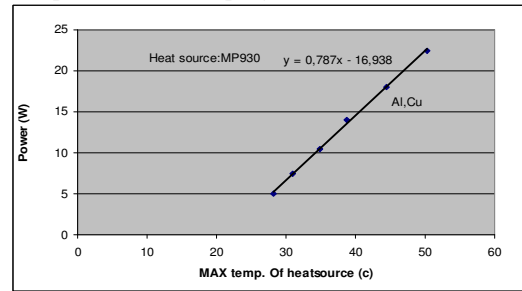
Graph 2: Relative performance MP930
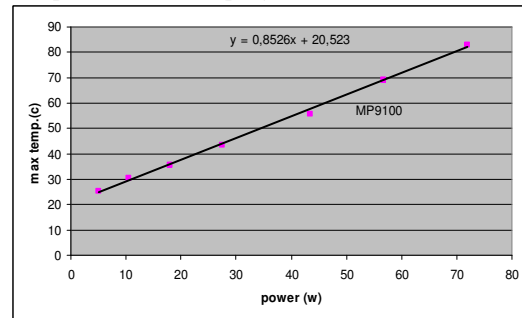
Graph 3: Relative performance MP9100
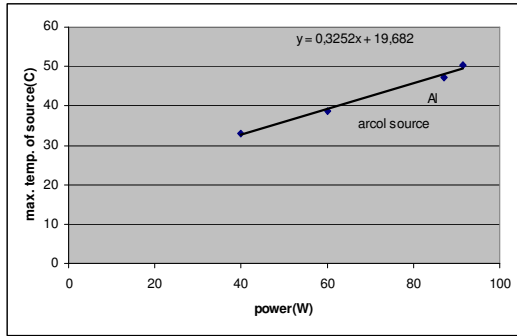
Graph 4: Relative performance Arcol (100-200w)

7.2.2 Heat transfer coefficient (h)

In the next table, h is accounted for several heat sources.

	Source	q/ΔT (^{0}C/W)	$A_{sour\text{-}area}$ (m^2)	h (W/ m^2K)
1	MP925	2.17	13.9E-02	3.3
2	MP930	1.25	13.9E-02	5.76
3	MP100	0.8	13.9E-02	9.1
4	Arcol(100-200)	0.33	13.9E-02	21.6

Table 3: Heat transfer coefficient for some heat sources

7.2.3 Reynolds number

Reynolds number is calculated by measuring the average air velocity at a distance about 13mm from a fan that is fitted in the pipe. At this distance of the fan the air velocity at variety of radial distances is measured.

u (m/s)	υ	D	T	Re
4.33	15.89×10^{-6}	98×10^{-3}	22	≈26000

Table4: Calculating the Reynolds number

7.2.4 Radial velocity profile

Radial flow velocity is measured experimentally inside a duct at some points from one end of the pipe where an axial fan is mounted.

Several holes are arranged at different distances along the pipe to measure the flow velocity by measurement equipments. When the measurement of the flow is intended at a particular point then the other holes are hold closed. At any constant point from the fan several measurement are performed to evaluate the radial velocity at that point.

The developing of airflow velocity versus the radial distance in the duct and at different distances of the fan is schematically demonstrated on the graphs below.
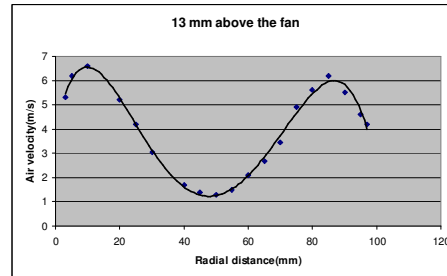
Graph 5: Air velocity versus the radial distance at 13 mm above the fan in a pipe
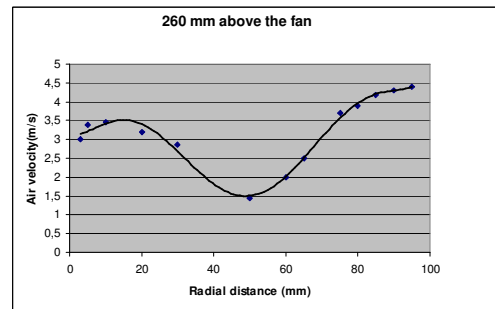
Graph 6: Air velocity versus the radial distance at 260 mm above the fan in a pipe
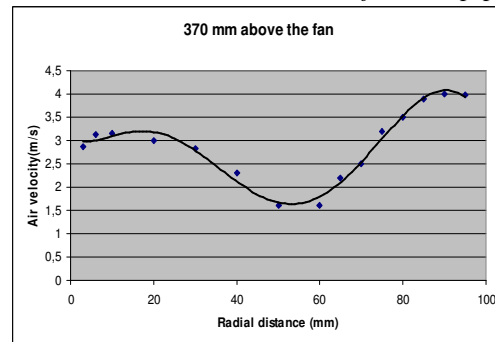
Graph 7: Air velocity versus the radial distance at 370 mm above the fan in a pipe
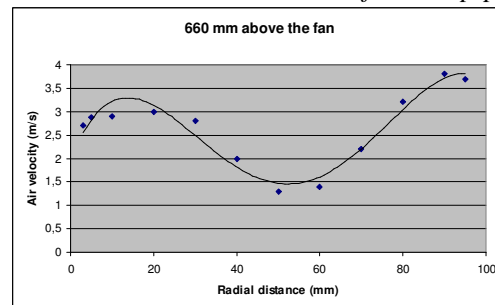
Graph 8: Air velocity versus the radial distance at 660 mm above the fan in a pipe

7.2.5   Dynamic pressure

The dynamic pressure is measured at about 13 mm above the fan. It is worthwhile to mention that these values need to be calibrated and turns into the pressure units. The objective is not to find the exact value of dynamic pressure but to find the relation between these values at the radial distance.
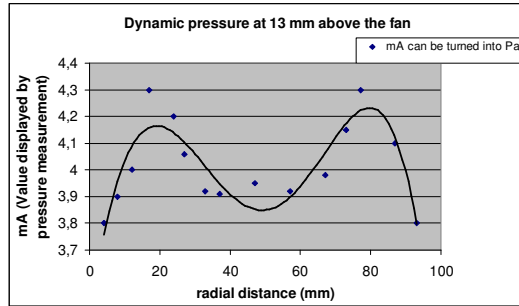
Graph 9: Dynamic pressure of the airflow at 13mm above the fan in the pipe

8. Discussion

The numerical simulation turns out that the flat plate copper heatsink has better thermal dissipation capability than the aluminium type. Additionally, the numerical study reveals the advantages of copper over aluminium with respect to heat spreading resistance. Copper has a significant lower thermal spreading resistance through the base plate in compared to aluminium. At higher heat fluxes this negative effect is substantial.
According to fig.4A and fig.4B the rate of heat spreading on the base of the heatsink is lower for the aluminium type. When the heat spreading through the base is poor therefore, the temperature difference between the base and the fins located at the distances further away from the centre decreases appreciably. Consequently the rate of heat transfer to these fins diminishes.
A warmer hot spot at the centre of the base where the heat source is attached is the next consequence of this effect.
However, the two analogous models are built in the Gambit framework and not practically. Production of such a heatsink by copper and in the same

manufacturing process route used for fabrication of aluminium heatsink would be prohibitively expensive. These factors are observed to design a mechanical heatsink with another perspective.
The new design for copper heatsink is proposed to avoid the aluminium production process approach.

The intension is to intensify the rate of heat transfer from the source through the fins. A solution is may be directly attachment of the fins to the heat source. The purpose is satisfied when the fins have direct contact without any intermediate, which generate the thermal resistance, with the heat source. The proposed design establishes the direct contact between the fins and the source.

Additionally, this component can be fabricated using existing low cost copper-friendly manufacturing technology as opposed to mimicking more common designs that optimized for aluminium.

8.1 Design optimization

Optimization is performed to improve the thermal characteristic of the heatsink. A particular type of heat source is adopted through the optimizations.
The design is improved and optimized experimentally.
Optimization initiated with a heatsink with 60 fins that are about twice as long as the common cast fins. Further optimization was performed for increasing the heat transfer coefficient. This parameter is not a function of only surface area and temperature difference (ΔT). Air velocity and pressure drop are two important parameters that affect the heat transfer coefficient and are dependent on the fin spacing. To this purpose the number of fins in optimization is reduced but their sizes are remained constant. The two advantage of this response are

respectively decreasing the weight and increasing the heat transfer coefficient. The optimization is summarized in the table (5).

	A$_{sour. area}$	q/ΔT	h	comments
1	↑	−	↓	Weight is increased
2	↑	↑	↑↓ −	Fin number& weight increases.for option is very good, − is good and ↓bad option
3	↓	−	↑	Fin number and weight is reduced but perfor. Is still constant
4	↓	↑	↑	Fin number & weight is reduced. Perfor. Is enhanced.
5	−	↑	↑	Higher air velocity

Table 5: Summary of heatsink optimization
The arrows and line applied in the table5 are explained as below

Trends: Increasing: ↑ *decreasing*: ↓ *no change:* −

Interpretation of the first optimization is that the surface area is increased by adding the fins but without any change in the thermal identity of the heatsink. Other consequences are respectively decreasing the fin spacing increasing the weight. The heat transfer coefficient drops due to increased flow bypass in the following of the decreasing the fin spacing. Therefore any increasing the surface area may not be a persistent solution.

8.2 Optimization by velocity profile

Specifying the airflow profile after the axial fan was important initially to understand whether which parts of heatsink was best and worst subjected to airflow. Radial velocity at different distances from a fan located at one end of a pipe is measured experimentally.
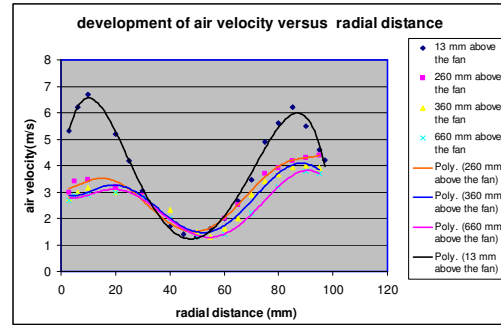
Graph 10: Summary of air flow velocties graphs
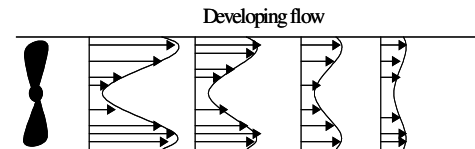
Figure 5:Development of air velocity profile for the axial fan in a pipe at the developing flow zone

The dynamic pressure measured at radius distances and 13 mm above the fan is also agreed with the velocity profile presented above. The development of the velocity profile for both developing and developed zones may be supposed as below:
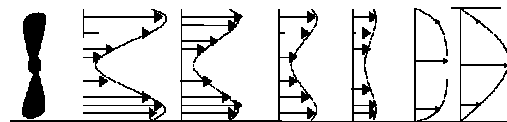
Figure 6: Air velocity profile for developing and developed flow in a duct equipped with an axial fan

Therefore the analytical correlations allocated for computing the radial velocity by equations 5 and 6 are not applicable in developing zone of airflow from an axial fan.

The treatment of flow velocity profile at different zones of the airflow along the pipe when utilizing an axial fan aids to exposure the under pressures and stream path.

Velocity profile turns out that at centre of the stream in the developing zone an under pressure develops which diminishes as the flow is progressing.

The middle zone of the sinks is the hottest part but according to air velocity

profile the best local heat transfer coefficient is gained at both sides of the centre in which the flow velocity is highest. To avoid any replacement of the fan to find the optimum fan location [6] above the sink, which is not desirable because it tends to increase the volume of the Compaq (fan plus sink), the fin design is instead improved in agreed with the velocity profile.

As shown in figure 1 a hole is designed at centre of the fin which keep the middle part of the sink a little longer away from the fan, diminishes the flow bypass effect and also expose the middle part of the sink to the airflow.

8.3 Relative performance of the heatsinks

The size of the heat source is important in determining the thermal performance but it is not the only influencing variable in this purpose. Table 2 indicates that thermal capability of a heatsink is depended on the type of the heat source. Determining the thermal heat dissipation capability of a heatsink for a heat source by knowing its performance for another heat source is not reliable.

Heat transfer coefficient is also a criterion for performance and varies with the type of the applied heat source and is proportional to the reverse of the performance i.e. $q/\Delta T$ and surface area.

8.4 Validity of numerical analysis

Simulation is conducted at different flow velocity and heat fluxes. The results turns out that source temperature is increased at lower flow velocities and higher heat fluxes which is agree with analytical equations. The range of the maximum temperature of the heatsource computed by CFD is reasonable and is at the same range of the experimental approach and therefore the confidence of the simulation elevates as well. To ensure the results, simulations are performed several times. In order to ensure the validity of the numerical solution, the iteration allowed continuing after the first convergence until the residual curves reached a long horizontal straight path.

9. Conclusion

Accumulating the fins tightly on a small heat source and however, utilizing the proper fin spacing can be accomplished by using the free fins of copper material. The softness of copper satisfies this goal. Softness and flexibility of copper make it easier to increase the heat transfer area and simultaneously create more fin spacing

In the common ways for making the heatsinks no matter the kind of material there is a heat spreading resistance at the base of the heatsink. The advantage of this model is that the heat is distributed evenly through the fins. The softness property of copper gives us this opportunity to have larger fin spacing.

The weight of the heatsink also reduces as a result of elimination of the base.

Dynamic pressure and airflow velocity are highest along the tip of the blades and lowest in front of the hub of the fan. Those parts of the copper heatsink that are located in the face of the hub are also subjected to a less airflow.

The introduced copper fin in this paper is designed according to parameters such as spreading resistance, velocity profile, and copper properties.

Since the production process of the proposed heatsink is simple a low manufacturing cost would be expected.

The weight of this model is lighter in compare to the most powerful and lightest heatsinks.

10. Acknowledgement

11. References

1- Brucer R. Munson, Donald F. Young, Theodor H. Okishi, Fundamentals of fluid mechanics third edition,1998, John Wiley & Sons pages 211-240

2- Frank P. Incropera, David p. Dewitt, Fundamental of heat and mass transfer, fourth edition 1996, John Wiley & Sons page 284-300

3- Fluent 6 user's guide volume 2, December 2001, page

4- NASA Glenn Learning Technologies home page

5- J. P Holman, Heat transfer, SI Metric Edition 1989,McGRAW-HILL book company, page 43-50, 220-245

6- A. Devinsky, A. Bar-Cohen, M. Strelets, Thermofluid analysis of staggered and inline pin fin heatsinks, Daat research corp. university of Minnesota

7- Victor L. Streeter , E. Benjamin Wylie fluid mechanics 1983, McGraw-Hill book company page 88-100 , 195-198

8- Johnny S. Issa Alfonso Ortega, Experimental measurements of the flow and heat transfer of a square impinging on an array of square pin fins

9- Barry Dagan, Pin Fin Heatsinks Supply Compact Cooling Power , Cool Innovations Inc., Concord, Ontario, Canada

10- Owen Stevens, "Owen-made Jet Impingement Cooling": Part One - The Slot" - 11/20/03, Page 1 of 9

Attachments
Heat sources

Figure 7: Heat source MP930 (30W) (1.00 Ω)

Figure 8: Arcol heat source (100-200w) (2, 2 Ω)
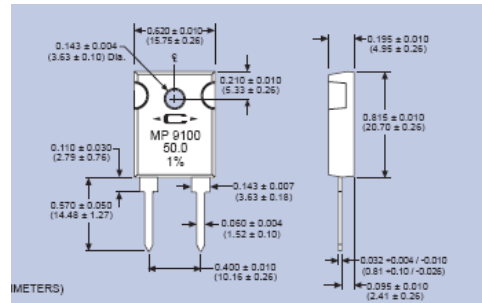
Figure 9: Heat source MP9100, (30W) (1.00 Ω)
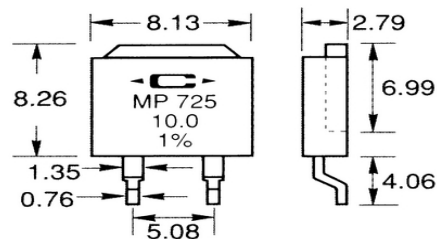
Figure 10: 25-watt heat source (MP725) (1.00Ω)